Supporting Information for

Subtly Regulating Layered Tin Chalcogenide Frameworks for Optimized Photo-Induced Carriers Separation

Chaozhuang Xue,*[a] Rui Li,[a] Wenhui Chen,[a] Yingying Zhang,[b] Ningning Zhang,*[a] Konggang Qu,[a] Ruiqing Li[c] and Huajun Yang*[b]

a School of Chemistry and Chemical Engineering, Liaocheng University, Liaocheng 252059, China.
E-mail: czxuelc@163.com, zhangningning@lcu.edu.cn
b School of Chemistry and Materials Science, Nanjing Normal University, 210023, Nanjing, China.
E-mail: huajunyang@nnu.edu.cn
c School of Textile and Clothing, Nantong University, Nantong 226019, China.

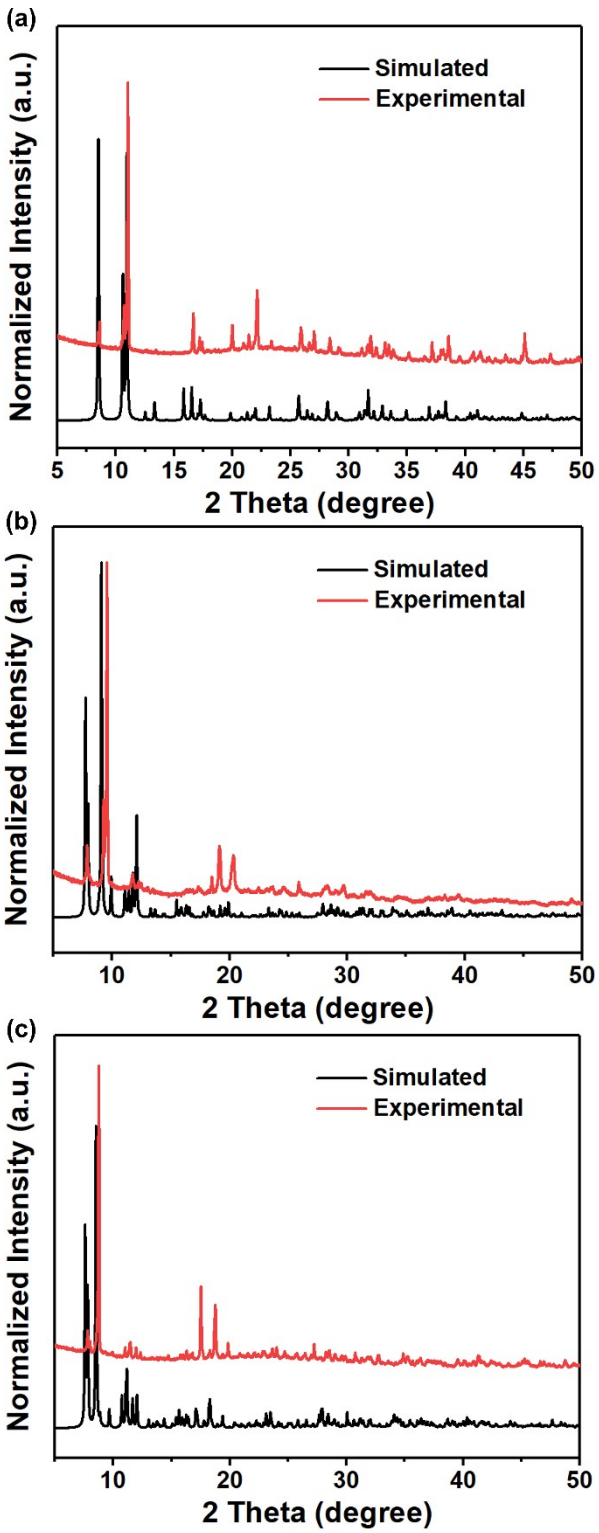

Fig. S1 Powder X-ray diffraction (PXRD) patterns for LTCF-1 (a), LTCF-2 (b) and LTCF-3 (c).

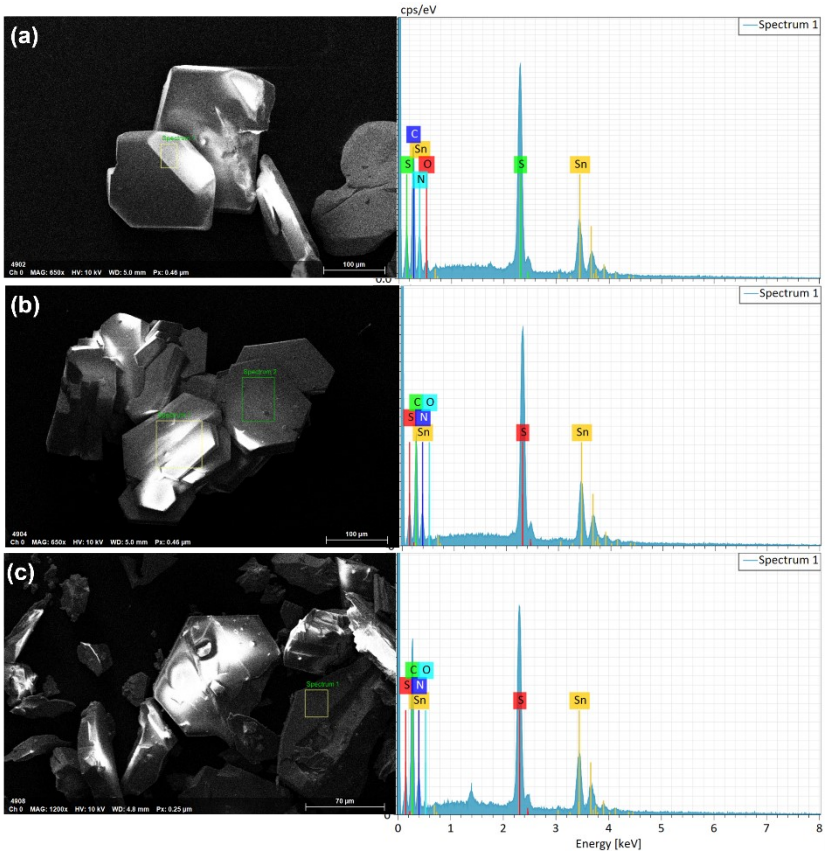

Fig. S2 SEM image and energy dispersive spectroscopy (EDS) for LTCF-1 (a), LTCF-2 (b) and LTCF-3 (c).

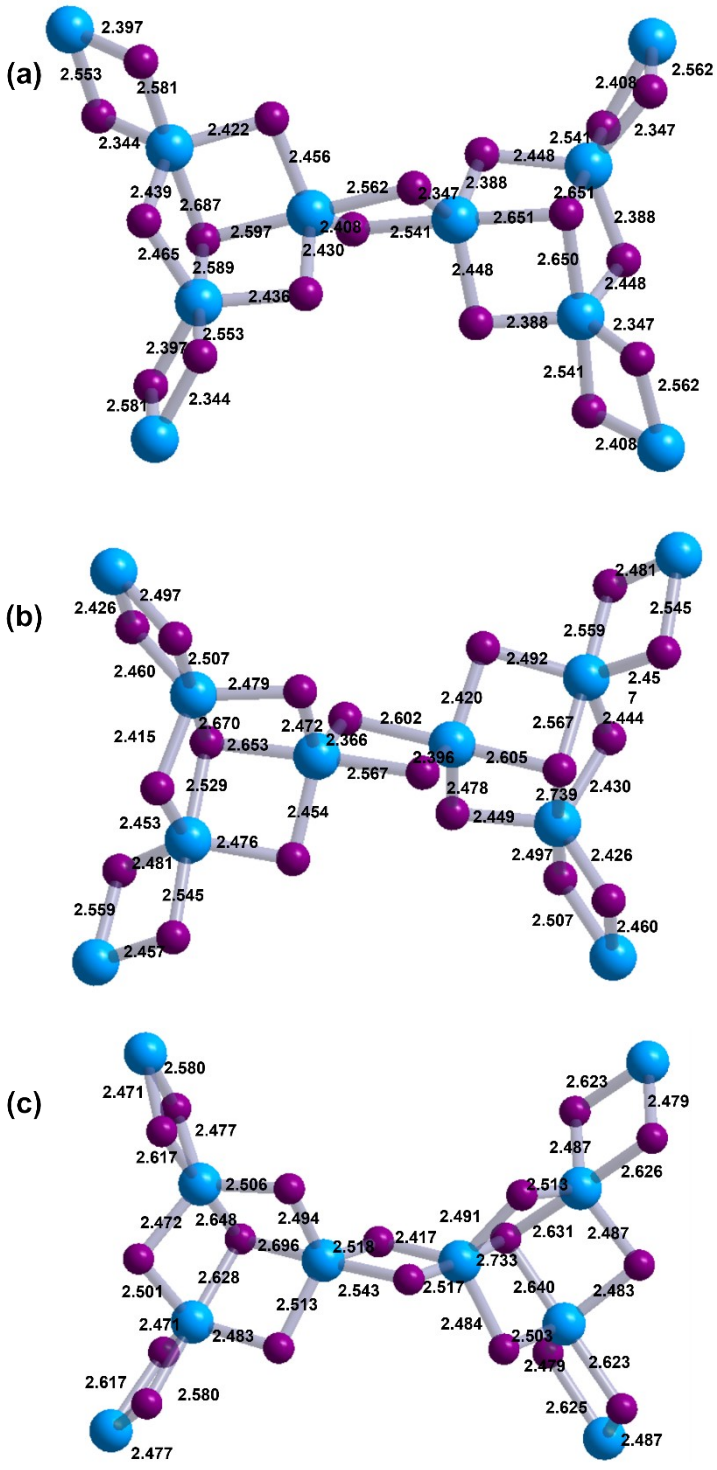

Fig. S3 The distribution of bond length in LTCF-1 (a), LTCF-2 (b) and LTCF-3 (c).

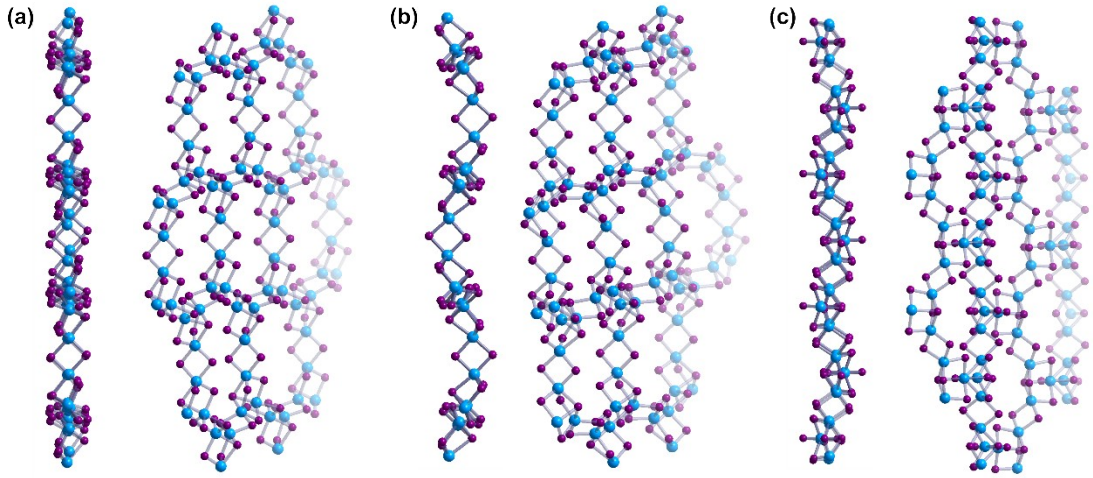

Fig. S4 Layered structures for LTCF-1 (a), LTCF-2 (b) and LTCF-3 (c) (blue atoms: Sn; purple atoms: S).

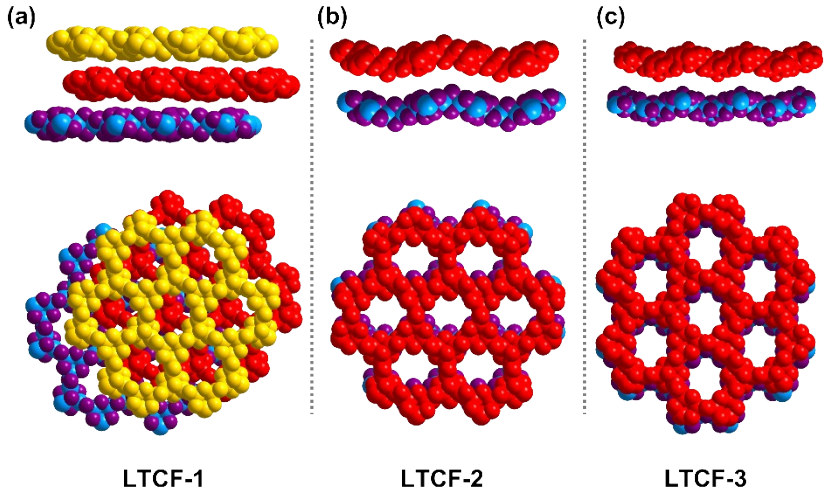

Fig. S5 The packed LTCFs with space-filling model (top: viewed from *a*-axis; bottom: viewed from *c*-axis).

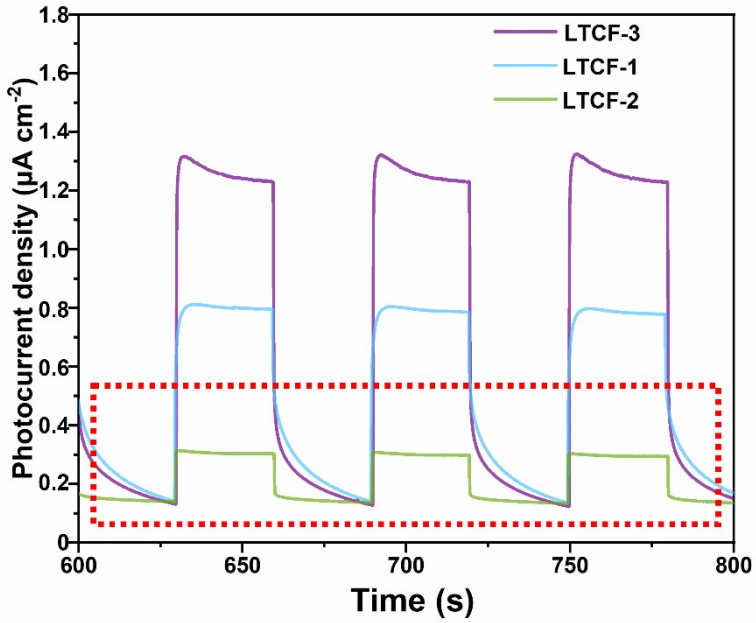

Fig. S6 Magnifying photoelectric response versus time curves (*J*–*t*) of LTCFs from fig. 2a, which show the smooth decrease of photocurrent density for LTCF-1 and 3 after light-off.

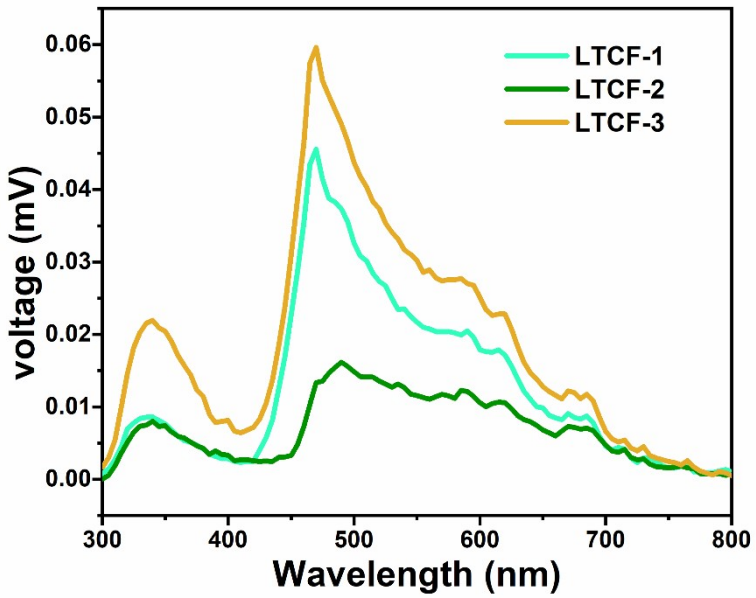

Fig. S7 Surface photovoltage (SPV) performance of three LTCFs under 0.6 V bias.

Table S1. Crystal data and structure refinement parameters for LTCFs.

Compounds	**LTCF-1**	**LTCF-2**	**LTCF-3**
Crystal system	Trigonal	Monoclinic	Monoclinic
Space group	$R\bar{3}$	$P\,21/c$	$P\,21/c$
Z	2	4	4
a (Å)	26.567	13.342	22.723
b (Å)	26.567	22.256	13.581
c (Å)	24.254	19.489	20.829
α (deg.)	90	90	90
β (deg.)	90	91.849	94.695
γ (deg.)	120	90	90
V (Å^3)	14825	5784.0	6406.5
GOF on F^2	1.994	1.456	1.433
R_1, wR_2 ($I>2\sigma(I)$)[a]	0.2263, 0.5235	0.1741, 0.4263	0.1866, 0.4534
R_1, wR_2 (all data)	0.2645, 0.5409	0.2183, 0.4487	0.2303, 0.4739

Note: [a] $R_1 = \sum||F_o|-|F_c||/\sum|F_o|$, $wR_2 = [\sum w(F_o^2-F_c^2)^2/\sum w\,(F_o^2)^2]^{1/2}$

Table S2. Elemental analysis (EA) results of three LTCFs.

Elements (wt.)	**N (%)**	**C (%)**	**H (%)**
Calculated for LTCF-1	6.76	20.28	2.92
Experimental for LTCF-1	6.48	21.73	4.55
Calculated for LTCF-2	6.76	20.28	2.92
Experimental for LTCF-2	6.64	19.87	4.32
Calculated for LTCF-3	6.33	24.43	3.64
Experimental for LTCF-3	6.12	22.52	4.48

1. Calculation of frontier orbitals

Calculations of structural fragment, extracted compound 3 crystal structure, were at the B3lyp/def2TZVP level, using the Gaussian 16 program[1]. The HOMO and LUMO results were analysed assistantly by Multiwfn[2].

2. Calculation of density of states (DOS)

The DOS were calculated using the CASTEP package[3]. The structural models for compounds 1–3 were built directly from the single-crystal X-ray diffraction data. The exchange-correlation energy was described by the PBE functional within the GGA[4,5]. The norm conserving pseudopotentials were chosen to modulate the electron-ion interaction[6,7]. The plane-wave cut off energy was 650 eV, and the threshold of 5×10-6 eV was set for the self-consistent field convergence of the total electronic energy. The Fermi level was selected as the reference and set to 0 eV by default. The smearing width was set to 0.05 eV for DOS. Other parameters were set to default values.

[1] Gaussian 16, Revision C.01, Frisch, M. J.; Trucks, G. W.; Schlegel, H. B.; Scuseria, G. E.; Robb, M. A.; Cheeseman, J. R.; Scalmani, G.; Barone, V.; Petersson, G. A.; Nakatsuji, H.; Li, X.; Caricato, M.; Marenich, A. V.; Bloino, J.; Janesko, B. G.; Gomperts, R.; Mennucci, B.; Hratchian, H. P.; Ortiz, J. V.; Izmaylov, A. F.; Sonnenberg, J. L.; Williams-Young, D.; Ding, F.; Lipparini, F.; Egidi, F.; Goings, J.; Peng, B.; Petrone, A.; Henderson, T.; Ranasinghe, D.; Zakrzewski, V. G.; Gao, J.; Rega, N.; Zheng, G.; Liang, W.; Hada, M.; Ehara, M.; Toyota, K.; Fukuda, R.; Hasegawa, J.; Ishida, M.; Nakajima, T.; Honda, Y.; Kitao, O.; Nakai, H.; Vreven, T.; Throssell, K.; Montgomery, J. A., Jr.; Peralta, J. E.; Ogliaro, F.; Bearpark, M. J.; Heyd, J. J.; Brothers, E. N.; Kudin, K. N.; Staroverov, V. N.; Keith, T. A.; Kobayashi, R.; Normand, J.; Raghavachari, K.; Rendell, A. P.; Burant, J. C.; Iyengar, S. S.; Tomasi, J.; Cossi, M.; Millam, J. M.; Klene, M.; Adamo, C.; Cammi, R.; Ochterski, J. W.; Martin, R. L.; Morokuma, K.; Farkas, O.; Foresman, J. B.; Fox, D. J. Gaussian, Inc., Wallingford CT, **2016**.

[2] Lu T, Chen FW. Multiwfn: A multifunctional wavefunction analyzer. *J Comput Chem* **2012**; 33: 580−592.

[3] Clark SJ, Segall MD, Pickard CJ, Hasnip PJ, Probert MIJ, Refson K, Payne MC. First principles methods using CASTEP. *Z Kristallogr-Cryst Mater* **2005**; 220: 567−570.

[4] Hammer B, Hansen LB, Norskov JK. Improved adsorption energetics within density-functional theory using revised Perdew-Burke-Ernzerhof functionals. *Phys Rev B Condens Matter Mater Phys* **1999**; 59: 7413−7421.

[5] Perdew JP, Wang Y. Accurate and simple analytic representation of the electron-gas correlation energy. *Phys Rev B Condens Matter Mater Phys* **1992**; 45: 13244−13249.

[6] Hamann DR, Schlüter M, Chiang C. Norm-Conserving Pseudopotentials. *Phys Rev Lett* **1979**; 43: 1494−1497.

[7] Lin JS, Qteish A, Payne MC, Heine V. Optimized and transferable nonlocal separable ab initio pseudopotentials. *Phys Rev B Condens Matter Mater Phys* **1993**; 47: 4174−4180.

3. Calculation of absorption property of LTCFs

The Vienna ab initio simulation package (VASP)[8,9] was employed to perform density functional theory (DFT) calculations within the generalized gradient approximation (GGA) using the Perdew-Burke-Ernzerhof (PBE)[10] function to describe the exchange correlation of electrons. The bulk UV light absorption spectrum of LTCF 1-3 were calculated. For the calculations, unit cells of LTCF 1-3 were used in this work. The projected augmented wave (PAW) potentials[11,12] were used to describe the ionic cores and take valence electrons into account using a plane wave basis set with a kinetic energy cutoff of 400eV. Partial occupancies of the Kohn-Sham orbitals were allowed using the Gaussian smearing method and a width of 0.05 eV. The electronic energy was considered self-consistent when the energy change was smaller than 10^{-6} eV. A geometry optimization was considered convergent when the force change was smaller than 0.01 eV/Å. Grimme's DFT-D3 methodology[13] was used to describe the dispersion interactions. The Brillouin zone was sampled using Monkhorst-Pack mesh k-points[14] with a reciprocal space resolution of $2\pi\times0.04$/Å. Since the atomic numbers in the three systems in Figure 1 are not identical, for better comparative analysis, the resulting absorptivity of the absorption spectrum was normalized.

[8] Kresse, G.; Furthmüller, J. Efficiency of Ab-Initio Total Energy Calculations for Metals and Semiconductors Using a Plane-Wave Basis Set. Comput. *Mater. Sci.* **1996**, 6, 15−50.
[9] Kresse, G.; Furthmüller, J. Efficient Iterative Schemes for Ab Initio Total-Energy Calculations Using a Plane-Wave Basis Set. *Phys. Rev. B* **1996**, 54, 11169−111 86.
[10] Perdew, J. P.; Burke, K.; Ernzerhof, M. Generalized Gradient Approximation Made Simple. *Phys. Rev. Lett.* **1996**, 77, 3865−3868.
[11] Kresse, G.; Joubert, D. From Ultrasoft Pseudopotentials to the Projector Augmented-Wave Method. *Phys. Rev. B* **1999**, 59, 1758-1775.
[12] Blöchl, P. E. Projector Augmented-Wave Method. *Phys. Rev. B* **1994**, 50, 17953−17979.
[13].Grimme, S.; Antony, J.; Ehrlich, S.; Krieg, H. *J. Chem. Phys.* **2010**, 132, 154104.
[14].H. J. Monkhorst and J. D. Pack, *Phys. Rev. B* **1976**, 13, 5188-5192.

Alert level A for crystallographic data of LTCF-1:

PLAT082_ALERT_2_A High R1 Value ..... 0.23 Report

PLAT084_ALERT_3_A High wR2 Value (i.e. > 0.25) ..... 0.54 Report

Alert level A for crystallographic data of LTCF-3:

PLAT084_ALERT_3_A High wR2 Value (i.e. > 0.25) ..... 0.47 Report

Response: All the alert A in LTCF-1 and LTCF-3 are caused by low resolution and high residual density (due to serious truncation effects of heavy metal atoms). The crystallinity of 2D layered chalcogenide usually is poor due the weak electrostatic interaction between negative layers and protonated amines. Several randomly-selected single crystals were tested to get better diffraction data, unfortunately, those data show similar crystallographic issue. Even so, we think that these alert level A in checkcif should not disturb the determination of crystal structure.